



Analysis of Apex Seal Friction Power Loss in Rotary Engines

Robert F. Handschuh
Glenn Research Center, Cleveland, Ohio

A. Karl Owen
U.S. Army Research Laboratory, Glenn Research Center, Cleveland, Ohio

NASA STI Program . . . in Profile

Since its founding, NASA has been dedicated to the advancement of aeronautics and space science. The NASA Scientific and Technical Information (STI) program plays a key part in helping NASA maintain this important role.

The NASA STI Program operates under the auspices of the Agency Chief Information Officer. It collects, organizes, provides for archiving, and disseminates NASA's STI. The NASA STI program provides access to the NASA Aeronautics and Space Database and its public interface, the NASA Technical Reports Server, thus providing one of the largest collections of aeronautical and space science STI in the world. Results are published in both non-NASA channels and by NASA in the NASA STI Report Series, which includes the following report types:

- **TECHNICAL PUBLICATION.** Reports of completed research or a major significant phase of research that present the results of NASA programs and include extensive data or theoretical analysis. Includes compilations of significant scientific and technical data and information deemed to be of continuing reference value. NASA counterpart of peer-reviewed formal professional papers but has less stringent limitations on manuscript length and extent of graphic presentations.
- **TECHNICAL MEMORANDUM.** Scientific and technical findings that are preliminary or of specialized interest, e.g., quick release reports, working papers, and bibliographies that contain minimal annotation. Does not contain extensive analysis.
- **CONTRACTOR REPORT.** Scientific and technical findings by NASA-sponsored contractors and grantees.

- **CONFERENCE PUBLICATION.** Collected papers from scientific and technical conferences, symposia, seminars, or other meetings sponsored or cosponsored by NASA.
- **SPECIAL PUBLICATION.** Scientific, technical, or historical information from NASA programs, projects, and missions, often concerned with subjects having substantial public interest.
- **TECHNICAL TRANSLATION.** English-language translations of foreign scientific and technical material pertinent to NASA's mission.

Specialized services also include creating custom thesauri, building customized databases, organizing and publishing research results.

For more information about the NASA STI program, see the following:

- Access the NASA STI program home page at <http://www.sti.nasa.gov>
- E-mail your question via the Internet to help@sti.nasa.gov
- Fax your question to the NASA STI Help Desk at 443-757-5803
- Telephone the NASA STI Help Desk at 443-757-5802
- Write to:
NASA Center for AeroSpace Information (CASI)
7115 Standard Drive
Hanover, MD 21076-1320



Analysis of Apex Seal Friction Power Loss in Rotary Engines

Robert F. Handschuh
Glenn Research Center, Cleveland, Ohio

A. Karl Owen
U.S. Army Research Laboratory, Glenn Research Center, Cleveland, Ohio

National Aeronautics and
Space Administration

Glenn Research Center
Cleveland, Ohio 44135

Level of Review: This material has been technically reviewed by technical management.

Available from

NASA Center for Aerospace Information
7115 Standard Drive
Hanover, MD 21076-1320

National Technical Information Service
5301 Shawnee Road
Alexandria, VA 22312

Available electronically at <http://gltrs.grc.nasa.gov>

Analysis of Apex Seal Friction Power Loss in Rotary Engines

Robert F. Handschuh
National Aeronautics and Space Administration
Glenn Research Center
Cleveland, Ohio 44135

A. Karl Owen
U.S. Army Research Laboratory
Glenn Research Center
Cleveland, Ohio 44135

Abstract

An analysis of the frictional losses from the apex seals in a rotary engine was developed. The modeling was initiated with a kinematic analysis of the rotary engine. Next a modern internal combustion engine analysis code was altered for use in a rotary engine to allow the calculation of the internal combustion pressure as a function of rotor rotation. Finally the forces from the spring, inertial, and combustion pressure on the seal were combined to provide the frictional horsepower assessment.

Introduction

The United States Army currently uses a 28.3 kW Wankel engine as the propulsion system for a small, unmanned aerial vehicle. In 2009 the Army Vehicle Technology Directorate at the Glenn Research Center initiated a fundamental research program intended to provide information and recommendations for improving the durability and performance of this engine. To properly assess any potential improvements, a quantitative understanding of the frictional horsepower requirements is required.

The rotary or Wankel engine is a fairly simple design of an internal combustion engine. There are no valves, camshaft, or connecting rods in this engine. The engine has two gears (one external that is fixed and one internal that rotates with the crankshaft journal), a rotor, a crankshaft, housings and support bearings. The number of parts to make an engine is very few in comparison to a typical internal combustion engine.

Due to the crankshaft rotating the rotor (triangle-shaped component) that meshes with an external gear fixed to the housing and floating via a bearing on the crankshaft journal, the crankshaft rotates three times for every one rotation of the rotor. Apex seals are on the tips of the rotor ends (there are three) and provide the sealing from one cavity to the next. The seals are very important to the performance of the engine.

The engine operates with the same four-stroke Otto cycle as a piston engine. The process is shown in Figure 1. In Figure 1 the four different strokes are numbered in the figure as intake, compression, power, and exhaust. Each cavity sweeps by the intake port, compresses the mixture, fires the mixture, then removes the exhaust every revolution of the rotor.

The rotor of this engine holds the seal components. The seals are a critical aspect of the engine maintaining its performance. A break down of the seal will lead to leakage between the cavities and contamination of the incoming fuel-air charge and a loss of power. The seal is rectangular in cross section and wear resistant. An example of the seal and contact spring are shown in Figure 2. The seal is two-piece with a split diagonal feature in the rotational axis direction to allow for proper sealing of the engine cavities at all operating (temperature) conditions.

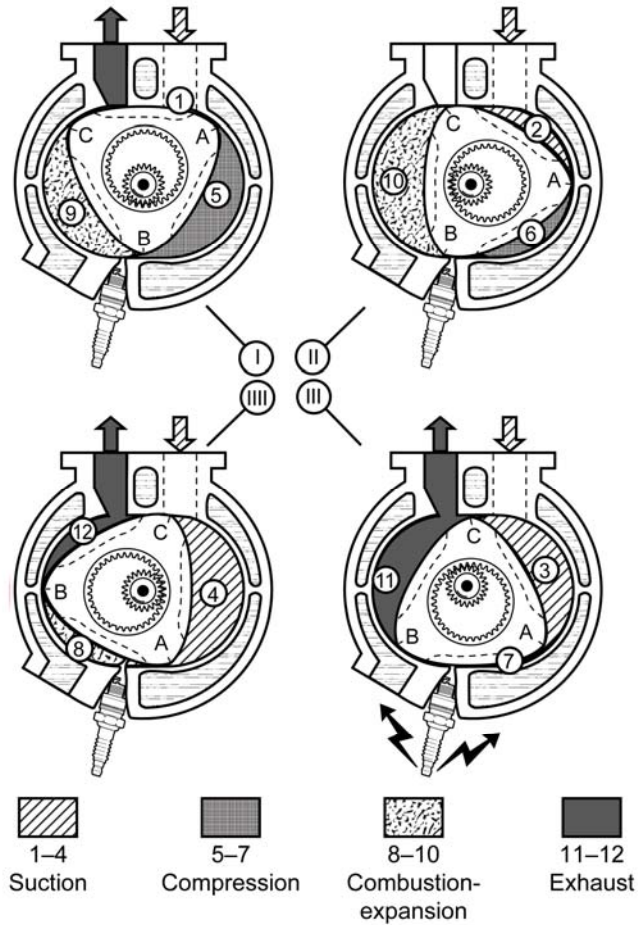


Figure 1.—Four-stroke operation of a rotary engine (Ref. 1).

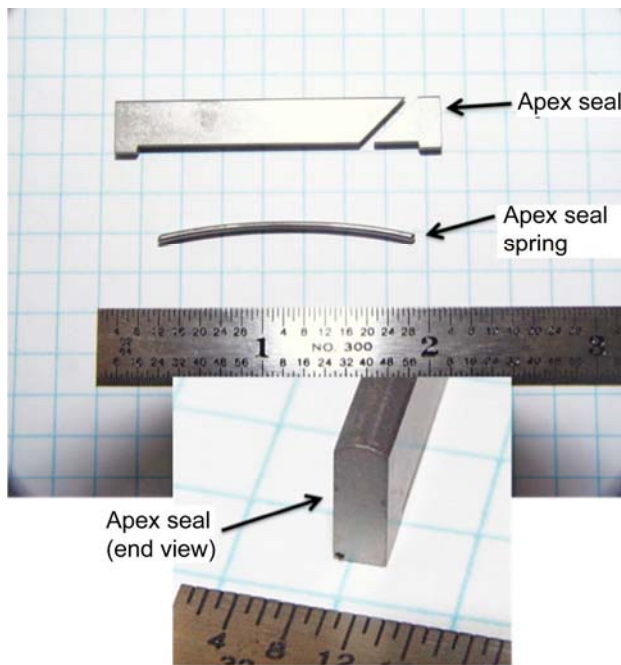


Figure 2.—Wankel engine apex seal components under study.

Kinematic Analysis

Dynamics of a Point on a Body With Translation and Rotation

A kinematic analysis of the rotary engine mechanism will now be described by first developing the general equations as given in References 2 to 4. The shape of the housing—or the path of the apex seal during operation is called an epitrochoid. A fixed coordinate system will be used to describe the position (path), velocity, and acceleration of a point at the apex of one of the rotor locations is shown in Figure 3 (there are three apex seals, 120° apart).

Coordinate system S_1 is the fixed frame of reference and coordinate system S_2 rotates with the rotor and point P is the location of the apex seal. O and O' are the centers for coordinate systems S_1 and S_2 , respectively. θ_1 and θ_2 are the rotation angles of the crankshaft and rotor in coordinate systems S_1 and S_2 , respectively. $\vec{\omega}_1$ and $\vec{\omega}_2$ are the rotational velocities of the crankshaft and rotor, respectively. \vec{R} is the position vector from coordinate system S_1 to S_2 . $\vec{\rho}$ is the position vector from O' to the apex seal. \vec{R} and $\vec{\rho}$ are fixed in magnitude but their direction is a function of the relationship between the coordinate systems.

The position vector, \vec{r} , for point P is given by

$$\vec{r} = \vec{R} + \vec{\rho} \quad (1)$$

Differentiating Equation (1) with respect to time results in the velocity with respect to the fixed coordinate system S_1 as

$$\vec{V} = \dot{\vec{r}} = \dot{\vec{R}} + \dot{\vec{\rho}} \quad (2)$$

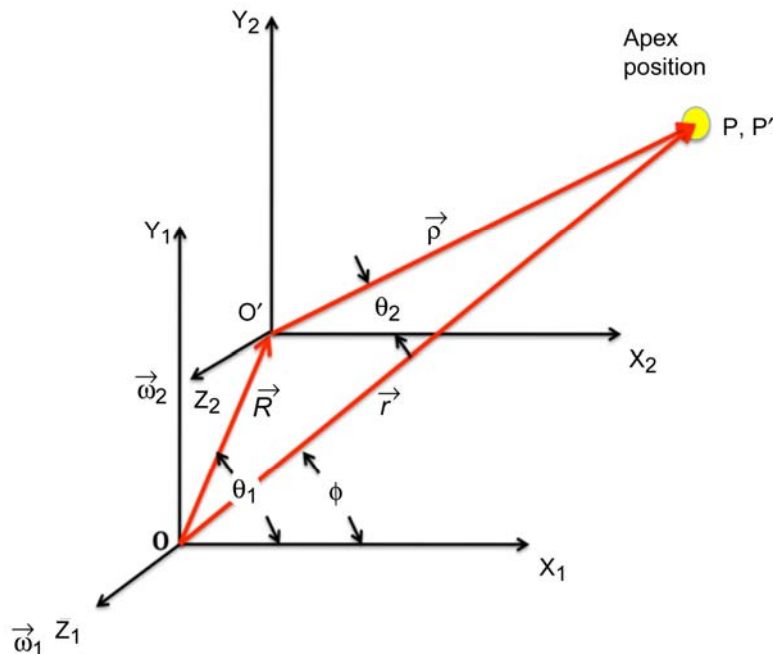


Figure 3.—Coordinate system used for kinematic analysis.

where

$$\vec{\rho} = (\vec{\rho})_r + \vec{\omega} \times \vec{\rho} \quad (3)$$

where $\vec{\omega}$ is the absolute rotation rate of coordinate system S_2 . Therefore, the apex velocity \vec{V} is given by

$$\vec{V} = \vec{R} + (\vec{\rho})_r + \vec{\omega} \times \vec{\rho} \quad (4)$$

Point P' is coincident with P in system S_2 but fixed in this coordinate system. \vec{R} is the absolute velocity of O' and $\vec{\omega} \times \vec{\rho}$ is the velocity of P' relative to O' as viewed by a non-rotating observer. Therefore

$\vec{R} + \vec{\omega} \times \vec{\rho}$ represents the absolute velocity of P' . The term $(\vec{\rho})_r$ is the velocity of P relative to O' as seen by an observer rotating with the S_2 coordinate system.

Next the acceleration will be described. Differentiating Equation (4) with respect to time provides the following

$$\frac{\partial}{\partial t}(\vec{V}) = \frac{\partial}{\partial t}(\vec{R}) + \frac{\partial}{\partial t}((\vec{\rho})_r) + \frac{\partial}{\partial t}(\vec{\omega} \times \vec{\rho}) \quad (5)$$

where the terms of equation become

$$\frac{\partial}{\partial t}(\vec{R}) = \vec{\ddot{R}}$$

$$\frac{\partial}{\partial t}((\vec{\rho})_r) = (\vec{\ddot{\rho}})_r + \vec{\omega} \times ((\vec{\rho})_r)$$

$$\frac{\partial}{\partial t}(\vec{\omega} \times \vec{\rho}) = \vec{\omega} \times \vec{\rho} + \vec{\omega} \times \vec{\rho} = \vec{\omega} \times \vec{\rho} + \vec{\omega} \times ((\vec{\rho})_r) + \vec{\omega} \times (\vec{\omega} \times \vec{\rho})$$

inserting these terms into Equation (5) results in the acceleration \vec{A} being given as

$$\vec{A} = \vec{\ddot{R}} + \vec{\omega} \times \vec{\rho} + \vec{\omega} \times (\vec{\omega} \times \vec{\rho}) + ((\vec{\ddot{\rho}})_r) + 2\vec{\omega} \times ((\vec{\rho})_r) \quad (6)$$

where

$\vec{\ddot{R}}$ is the absolute acceleration of O' , $\vec{\omega} \times \vec{\rho}$ and $\vec{\omega} \times (\vec{\omega} \times \vec{\rho})$ represent the acceleration of P' relative to O' as viewed from a non-rotating observer. In other words with $\vec{\omega} \times \vec{\rho}$ is the tangential acceleration and $\vec{\omega} \times (\vec{\omega} \times \vec{\rho})$ is the centripetal acceleration of P towards the axis of rotation through O' . Vector $((\vec{\ddot{\rho}})_r)$ is the acceleration of point P relative to the S_2 coordinate system as viewed by an observer moving with S_2 . Vector $2\vec{\omega} \times ((\vec{\rho})_r)$ is the Coriolis acceleration.

Application to a Rotary Engine

For the rotary engine the following are given as known due to the timing of the mechanism between the rotor, crankshaft and the internal-external gearing. In this engine a 30-tooth external gear is fixed to the housing. A 45-tooth internal gear rotates about the fixed external gear with the crankshaft offset equal to the center distance difference of the meshing external-internal gears. This results in a 3:1 angular and rotational relationship between the crankshaft and the rotor. In the analysis, the crankshaft speed and rotation relationships are then given as: $\theta_2 = \theta_1 / 3$ and $\omega_1 = \text{const}$, and $\omega_2 = \omega_1 / 3$.

The equation for the apex seal velocity becomes the following (since $((\vec{\rho})_r) = 0$; point P does not move relative to O' for a rotating observer)

$$\vec{V} = \vec{R} + \vec{\omega} \times \vec{\rho} \quad (7)$$

The acceleration is the following (since $\vec{\rho} = 0$, then $\ddot{\vec{\rho}} = 0$) Equation (6) becomes

$$\vec{A} = \vec{R} + \vec{\omega} \times (\vec{\omega} \times \vec{\rho}) \quad (8)$$

From Figure 3 the position vector for the apex seal is given as

$$\vec{r} = \begin{Bmatrix} |R| \cos \theta_1 + |\rho| \cos \theta_2 \\ |R| \sin \theta_1 + |\rho| \cos \theta_2 \\ 0 \end{Bmatrix} \quad (9)$$

and the velocity vector becomes

$$\vec{V} = \begin{Bmatrix} -\omega_1 |R| \sin \theta_1 - \omega_2 |\rho| \sin \theta_2 \\ \omega_1 |R| \cos \theta_1 + \omega_2 |\rho| \cos \theta_2 \\ 0 \end{Bmatrix} \quad (10)$$

finally the acceleration vector is given by

$$\vec{a} = \begin{Bmatrix} -\omega_1^2 |R| \cos \theta_1 - \omega_2^2 |\rho| \cos \theta_2 \\ -\omega_1^2 |R| \sin \theta_1 - \omega_2^2 |\rho| \sin \theta_2 \\ 0 \end{Bmatrix} \quad (11)$$

Using Equation (9) developed for the apex seal path for a given crankshaft offset and the distance from the rotor center to the apex seal location, the path the seal takes for one revolution is shown in Figure 4. This is approximately the same geometry as the static housing that the seal is in contact with during operation and will be assumed in this paper to be the path of the apex seal.

Next the seal velocity as a function of crankshaft rotation angle found from Equation (10) is given in Figure 5. The velocity of the seal is presented as that in the fixed coordinate system. The velocity is given for the engine crankshaft speed equal to 7800 rpm.

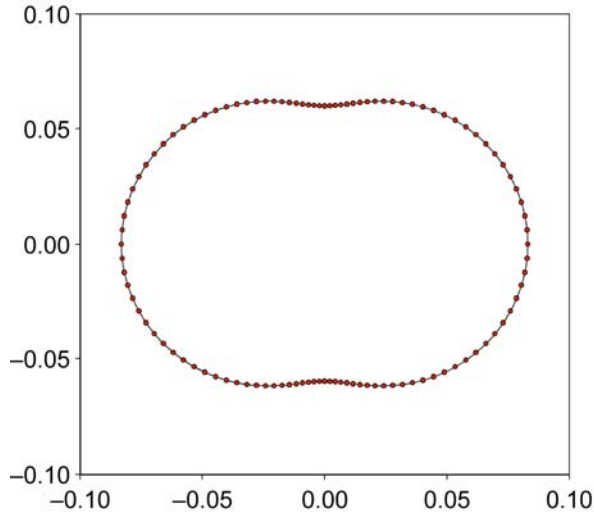


Figure 4.—Apex seal path.

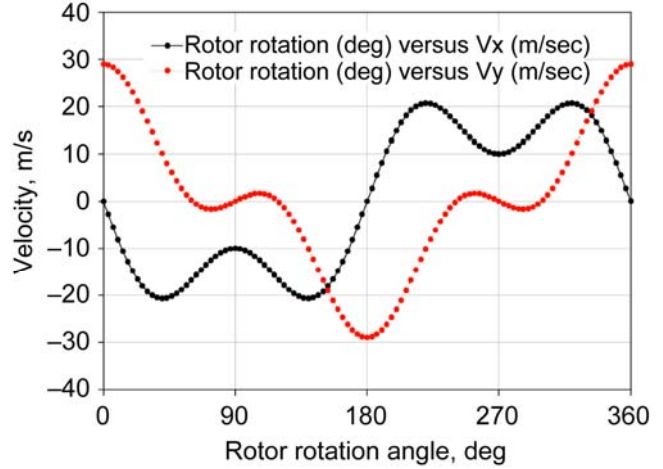


Figure 5.—Apex seal velocity as a function of crankshaft position angle (7800 rpm).

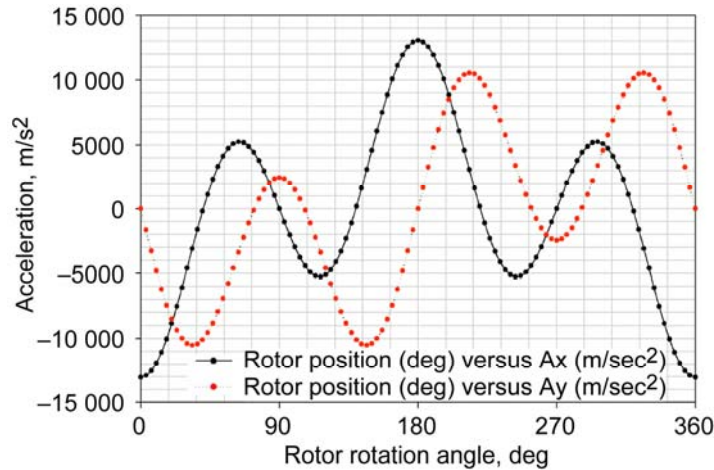


Figure 6.—Apex seal acceleration as a function of crankshaft position angle (7800 rpm).

Next the acceleration of the apex seal is presented by evaluating Equation (11) as a function of crankshaft rotation angle at 7800 rpm. The acceleration is also shown in the fixed coordinate directions (see Fig. 6).

The development so far has concentrated on the calculations made in the fixed coordinate system. At this point it would be useful to put the same calculation methodology into a coordinate system that is radial and transverse to that of the apex seal itself. This will be done via the coordinate system shown in Figure 7.

From Figure 7 the radial and transverse directions are along vector $\vec{\rho}$ and perpendicular to this vector, respectively. Therefore, to express the acceleration in terms of a radial and transverse direction, the acceleration vector must be transformed into these directions. This can be written as the following:

$$\begin{Bmatrix} a_{radial} \\ a_{transverse} \end{Bmatrix} = \begin{bmatrix} \cos\theta_2 & \sin\theta_2 \\ -\sin\theta_2 & \cos\theta_2 \end{bmatrix} \begin{Bmatrix} a_{x-fixed} \\ a_{y-fixed} \end{Bmatrix} \quad (12)$$

Using Equation (12) the acceleration shown in Figure 6 after transformation is shown in Figure 8.

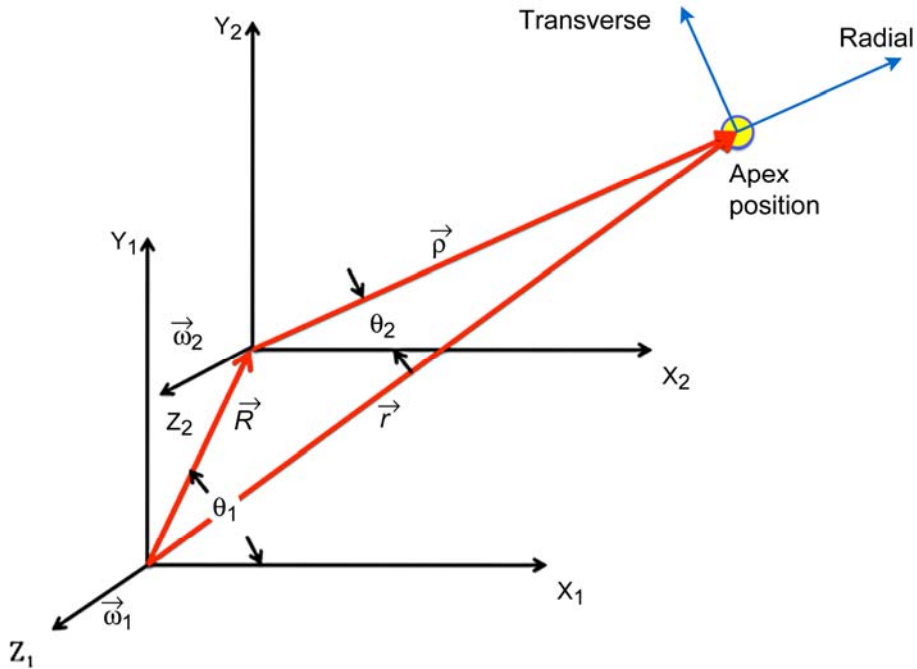


Figure 7.—Coordinate system for radial and transverse components for the apex seal.

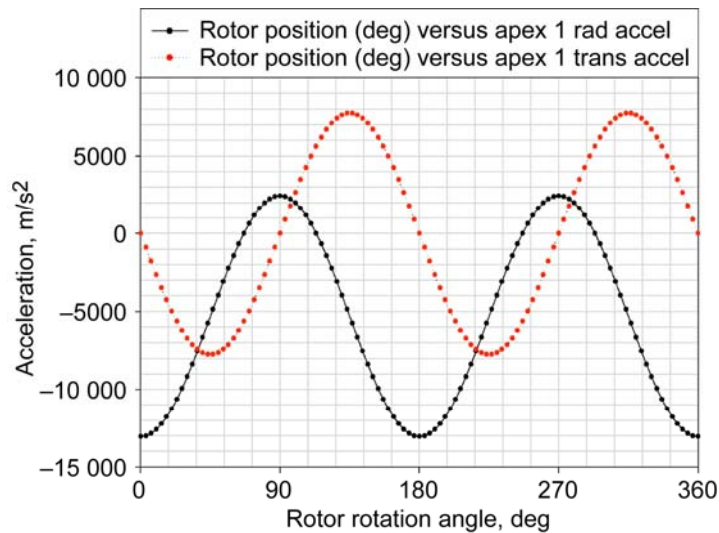


Figure 8.—Acceleration components in the radial and transverse apex seal directions (7800 rpm).

Combustion Modeling

To effectively analyze the friction torque developed by the rotor seals, the effects of combustion chamber pressure on the rotor and its seals must be included in the analysis. Limited experimental data of pressures inside a Wankel engine are available and no data for the particular engine in question are publically available. Therefore, the required information was generated analytically.

A widely-used commercial software package (Ref. 6) designed for performance calculations of an internal combustion engine was used to model this Wankel engine. These one-dimensional commercial

packages do not contain specific Wankel engine configurations. Because they are not configured to directly model the rotary configuration, a number of assumptions are required that qualify the accuracy of the results. Nonetheless, the results can be used to provide a reasonable initial assessment of engine performance until high-fidelity three-dimensional modeling and experimental results can be obtained.

The engine was modeled as a three cylinder 4-stroke reciprocating engine, as shown in Figure 9.

This configuration required the engine to operate at one-third to actual speed with an added gearbox to provide the rated rpm. In addition, the simulation package does not directly allow modeling of a carburetor; however standard procedure is to use a fuel injection module that is properly configured to represent the operation of a carburetor. Other physical geometry required by the model, such as intake and exhaust port geometry was measured from the engine and input to the model.

The following assumptions were made to assemble this model:

1. The model fuel consumption was input as the listed brake specific fuel consumption (BSFC) at maximum rpm.
2. Combustion was assumed stoichiometric.
3. Stroke was assumed to be the same as the eccentric offset and the bore was calculated to provide the same volume.
4. Top dead center clearance was used to adjust to the published compression ratio.
5. Compression versus crank angle was input using formulas provided by Reference 7.
6. Standard heat release (Weibe) and gas exchange models, as provided by the software, were used.

With these assumptions, the simulation friction model was adjusted to result in the appropriate power output.

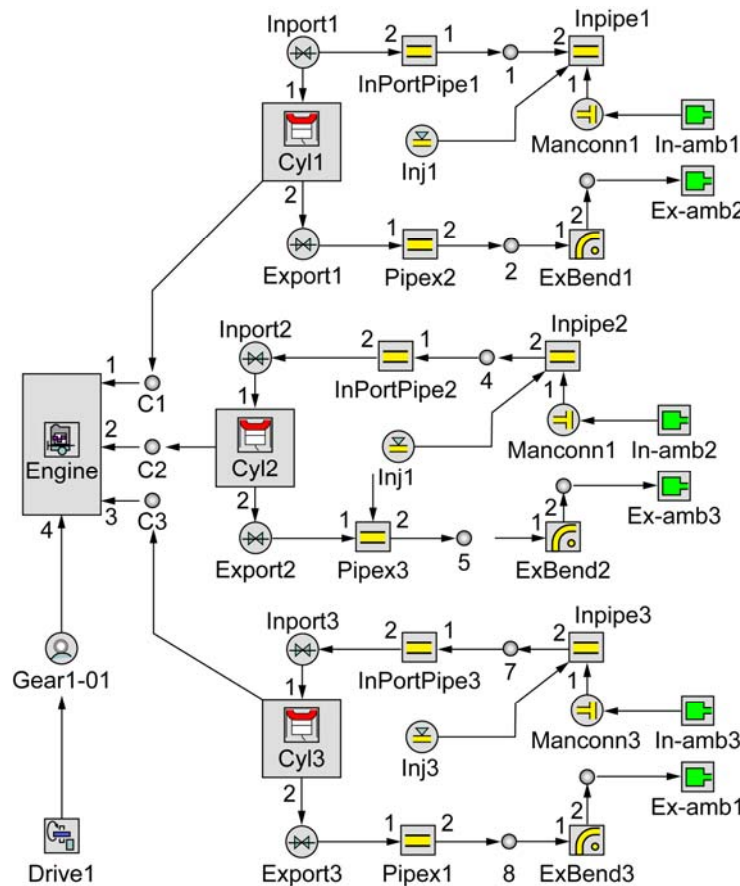


Figure 9.—Schematic of simulation model.

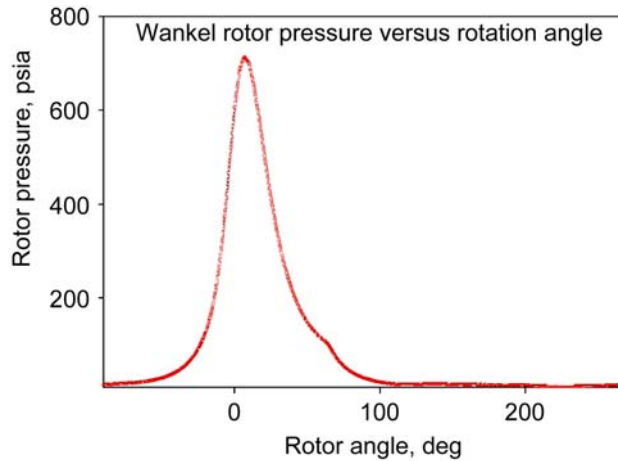


Figure 10.—Rotor pressure for one cavity as a function of rotor angle.

These assumptions likely deviate significantly from the actual operation of the engine as this configuration most certainly has a different gas exchange characteristic than a typical 2-stroke and certainly the combustion characteristics in the very elongated combustion chamber with a “piston” moving horizontally as well as vertically will deviate from that of a standard piston.

The resulting pressure trace versus crank angle is shown below in Figure 10. The rotor at 0° represents top dead center. In the coordinate system described earlier in this paper the orientation of the location of top dead center was transformed to the coordinate description shown in Figure 2 such that pressure from the cavity leading apex seal 1 (Cavity 3) was shifted 30° ahead. This made top dead center equal to when apex seal 1 had rotated 30° (or the crankshaft had rotated 90°).

Combination of Loads

The rotary engine, when operating, has three different loads being applied to the apex seal that result in a frictional (parasitic) drag of the apex seals on the stationary housing. There is a spring force from a leaf-type spring located under the apex seal, the inertial force due to the mass of the seal being accelerated around the epitrochoid path and the combustion pressure forces. The loading is shown schematically in Figure 11. The spring force was experimentally measured for the system under study, and resulted in a force of approximately 44.5 N at approximately half of its compressed height. Also the mass of the seal itself was found to be 8.36 g. In the model developed the spring force was assumed to be constant and the inertial force due to the mass of the apex seal was found based on the analysis conducted above.

Next the combustion loading on the seal had to be interpreted. As shown in Figure 10, the combustion loading pressure is very dependent on the rotor angle position. Each lobe of the rotor experiences this loading per revolution.

The cavity pressure affects the apex seals before and after the seal location as shown in Figure 11. Therefore the pressure on each side of the apex seal was determined during the rotor rotation process.

The cavity pressures are shown in Figure 12 as a function of rotor rotation angle.

Using Figure 13 the radial and transverse forces on the apex seal can be found. The seal is assumed to be of length, L , in the third dimension and the pressure loading around the seal-housing contact location is assumed to be negligible. Also, the seal is assumed to remain in contact on the backside of the rotor-seal interface during the entire apex seal traverse of the rotor housing.

The forces in the radial direction are given by the following for apex seal 1:

$$\sum F_r = m_{seal} S_r \quad (13)$$

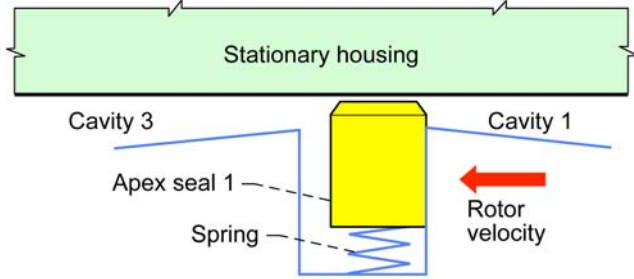


Figure 11.—Apex seal arrangement.

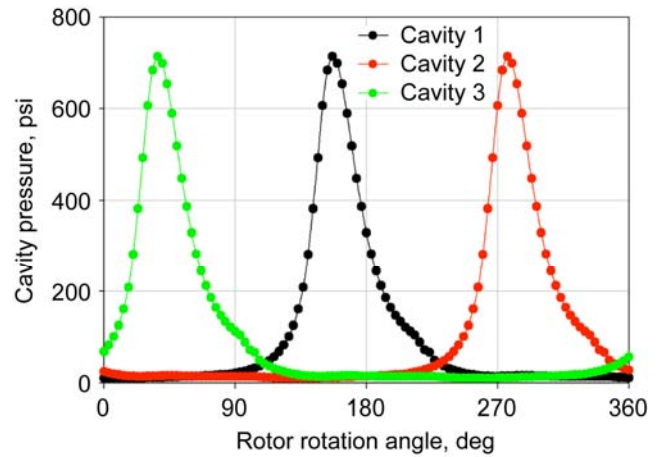


Figure 12.—Cavity pressure as a function of rotor rotation position.

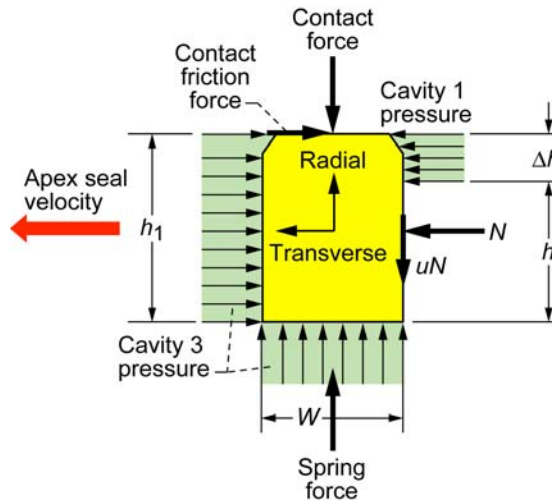


Figure 13.—Apex seal 1 free body diagram.

From Figure 13 this becomes:

$$-F_{cont} + F_{spring} + P_{cav3}WL - \mu N = m_{seal}S_r \quad (14)$$

This can be rearranged to be:

$$F_{cont} = -m_{seal}S_r + F_{spring} + P_{cav3}WL - \mu N \quad (15)$$

The forces in the transverse direction are given by:

$$\sum F_t = m_{seal}S_t \quad (16)$$

Using Figure 13 this becomes:

$$-\mu F_{cont} - P_{cav3}h_1L + P_{cav1}\Delta hL + N = m_{seal}S_t \quad (17)$$

Solving Equation (17) for N results in the following:

$$N = m_{seal} S_t + L(P_{cav3} h_1 - P_{cav1} \Delta h) + \mu F_{cont} \quad (18)$$

Inserting Equation (18) into Equation (15) and rearranging results in

$$F_{cont} = \left(\frac{1}{1 + \mu^2} \right) \left\{ -m_{seal} (a_{radial} + \mu a_{transverse}) + P_{cav3} (WL - \mu L h_1) + F_{spring} + \mu L P_{cav1} \Delta h \right\} \quad (19)$$

Using Figure 14 the friction torque can be found as apex seal 1:

$$T_{seal\#1} = r \mu F_{cont} \cos \gamma \quad (20)$$

where γ is given by:

$$\gamma = \cos^{-1} \left(\frac{|\vec{r}^2| + |\vec{\rho}^2| - |\vec{R}^2|}{2|\vec{r}||\vec{\rho}|} \right) \quad (21)$$

and the power lost due to seal friction as a function of apex rotation location as:

$$P_{Total} = \sum_{i=1}^3 T_{seal\#i} \omega \quad (22)$$

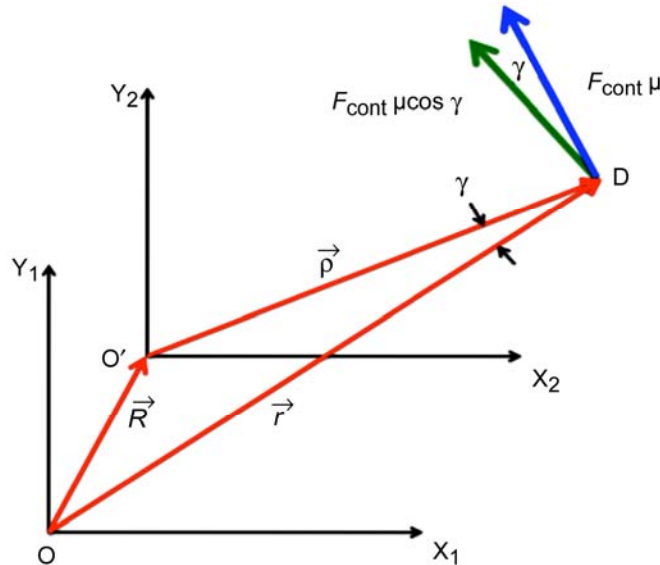


Figure 14.—Friction torque shown relative to crankshaft centerline.

Analytical Results

The analysis developed in this paper will now be applied first to a single seal and then to the entire three-seal engine configuration. The main parameters that will be investigated will be the effect of friction and crankshaft rotational speeds.

First a single seal will be investigated. In Figure 15 the seal contact force and cavity pressures (around apex seal 1) are shown as a function of rotor rotation angle. The crankshaft speed was maintained at 7800 rpm with the friction coefficient set to 0.04 and held constant. At this point the coefficient of friction chosen requires some discussion. Obviously this effect is related to many operational characteristics not contained in this analysis. These characteristics include sliding speed, contact load, temperature, pressure, etc. The assumption of using the friction coefficient equal to 0.04 is similar to the contact friction between smooth surface metallic components as described in Reference 8. Investigating this parameter is important enough to warrant a separate investigation.

Using the information previously discussed permits the analysis of a single seal. Figure 15 shows that the large contact force between the apex seal and the stationary housing is directly linked to the cavity pressure ahead of the apex seal.

If the other two seals are added to this diagram, the total friction power loss for a given speed and friction coefficient can be found. The results are shown in Figure 16. Here the frictional affects range from approximately 900 to 2200 W during a three crankshaft revolution period (one rotor rotation).

Also, the information shown in Figure 16 can be displayed one component at a time. Shown in Figure 17 is the total power loss for all three-apex seals, for each component and the total.

Next in Figure 18, the effect of friction coefficient on the frictional power loss is shown. At this point the actual friction coefficient is unknown, but believed to be between 0.01 and 0.04. In the analysis conducted this value was kept constant. In reality, this value would vary and be a function of the loading, speed, temperature and other conditions not accounted for in this analysis.

The final comparison provided is the effect of crankshaft rotation speed on the frictional power loss. In Figure 19 the analysis was conducted for three speeds (1000, 4000, and 7800 rpm). The friction coefficient was held constant at 0.04. As shown in the figure, speed has a strong influence on the frictional power loss found.

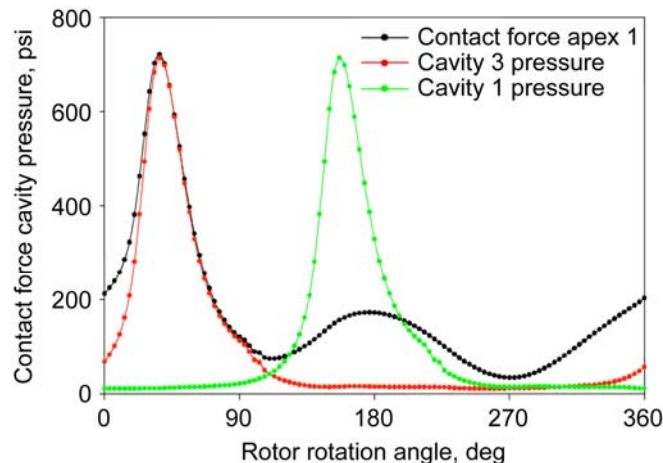


Figure 15.—Apex seal 1 contact force and cavity pressures as a function of rotor rotation angle.

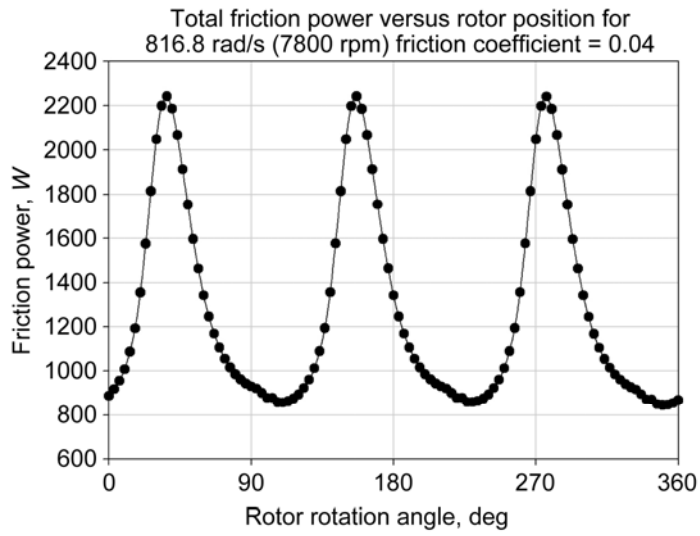


Figure 16.—Total friction power loss as a function of crankshaft position angle.

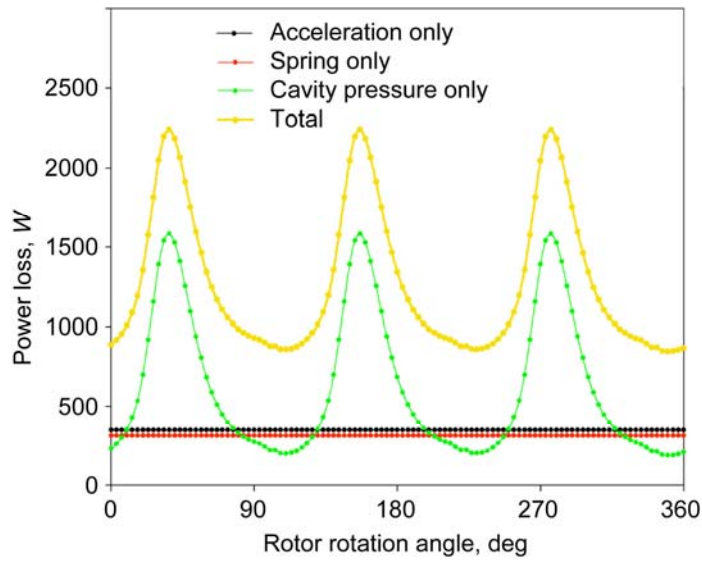


Figure 17.—Power loss components and total for 7800 rpm and a friction coefficient equal to 0.04 for all three apex seals.

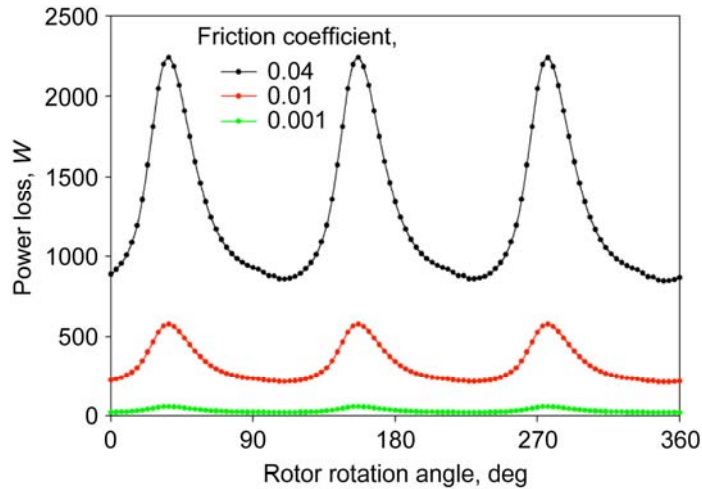


Figure 18.—Effect of friction coefficient assumed at 7800 rpm crankshaft speed.

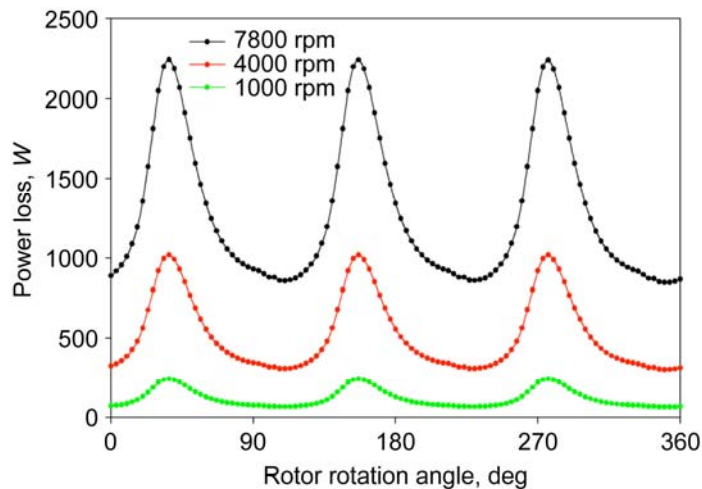


Figure 19.—Effect of crankshaft rotational speed on the total friction power loss (friction coefficient = 0.04).

Conclusions

Based on the results found in this study the following conclusions can be drawn:

1. The dynamics of the rotor of a rotary engine have been described. The analytical treatment developed can be utilized for any rotary engine given the crankshaft, rotor design parameters, and combustion pressure. The apex seal path, velocity and acceleration were found.
2. A combustion modeling computer code was utilized to predict the cavity pressure during the four-stroke simulation. The combustion pressure as a function of rotor position was used in the analysis.
3. The effects of inertial, apex seal spring, and combustion pressure were analyzed separately and combined to determine the parasitic, friction losses in the rotary engine under study.
4. Friction coefficient and crankshaft speed effects were investigated. Both factors had a drastic effect on the resultant power loss predicted.

References

1. C. Vilman, Deformation Analysis of Rotary Combustion Engine Housings, Michigan Technical University, NASA CR-188187, 1991.
2. D. Greenwood, Principles of Dynamics, Prentice-Hall Inc., 1988.
3. R. Hinkle, Kinematics of Machines, Second Edition, Prentice-Hall, Inc., 1960.
4. H. Mabie and F. Ocvirk, Mechanisms and Dynamics of Machinery, Third Edition, John Wiley & Sons, 1975.
5. R. Ansdale and D. Lockley, The Wankel RC Engine, Design and Performance, A.S. Barnes and Company, 1st Edition, 1969.
6. GT-Suite, V7.0.0, November, 2009.
7. K. Yamamoto, Rotary Engine, Sankaido Co., Ltd., 1981.
8. P. Andersson, J. Tamminen, and C.-E. Sandstrom, Piston Ring Tribology, A Literature Review, VTT Research Notes, 2002.

REPORT DOCUMENTATION PAGE			Form Approved OMB No. 0704-0188		
<p>The public reporting burden for this collection of information is estimated to average 1 hour per response, including the time for reviewing instructions, searching existing data sources, gathering and maintaining the data needed, and completing and reviewing the collection of information. Send comments regarding this burden estimate or any other aspect of this collection of information, including suggestions for reducing this burden, to Department of Defense, Washington Headquarters Services, Directorate for Information Operations and Reports (0704-0188), 1215 Jefferson Davis Highway, Suite 1204, Arlington, VA 22202-4302. Respondents should be aware that notwithstanding any other provision of law, no person shall be subject to any penalty for failing to comply with a collection of information if it does not display a currently valid OMB control number.</p> <p>PLEASE DO NOT RETURN YOUR FORM TO THE ABOVE ADDRESS.</p>					
1. REPORT DATE (DD-MM-YYYY) 01-09-2010		2. REPORT TYPE Technical Memorandum		3. DATES COVERED (From - To)	
4. TITLE AND SUBTITLE Analysis of Apex Seal Friction Power Loss in Rotary Engines			5a. CONTRACT NUMBER		
			5b. GRANT NUMBER		
			5c. PROGRAM ELEMENT NUMBER		
6. AUTHOR(S) Handschuh, Robert, F.; Owen, A., Karl			5d. PROJECT NUMBER		
			5e. TASK NUMBER		
			5f. WORK UNIT NUMBER WBS 877868.02.07.03.01.01.01		
7. PERFORMING ORGANIZATION NAME(S) AND ADDRESS(ES) National Aeronautics and Space Administration John H. Glenn Research Center at Lewis Field Cleveland, Ohio 44135-3191			8. PERFORMING ORGANIZATION REPORT NUMBER E-17289		
9. SPONSORING/MONITORING AGENCY NAME(S) AND ADDRESS(ES) National Aeronautics and Space Administration Washington, DC 20546-0001 and U.S. Army Research Laboratory Adelphi, Maryland 20783-1145			10. SPONSORING/MONITOR'S ACRONYM(S) NASA, ARL		
			11. SPONSORING/MONITORING REPORT NUMBER NASA/TM-2010-216353; ARL-TR-5162		
12. DISTRIBUTION/AVAILABILITY STATEMENT Unclassified-Unlimited Subject Category: 37 Available electronically at http://gltrs.grc.nasa.gov This publication is available from the NASA Center for AeroSpace Information, 443-757-5802					
13. SUPPLEMENTARY NOTES					
14. ABSTRACT An analysis of the frictional losses from the apex seals in a rotary engine was developed. The modeling was initiated with a kinematic analysis of the rotary engine. Next a modern internal combustion engine analysis code was altered for use in a rotary engine to allow the calculation of the internal combustion pressure as a function of rotor rotation. Finally the forces from the spring, inertial, and combustion pressure on the seal were combined to provide the frictional horsepower assessment.					
15. SUBJECT TERMS Internal combustion engines; Apex seals; Dynamics					
16. SECURITY CLASSIFICATION OF:			17. LIMITATION OF ABSTRACT	18. NUMBER OF PAGES	19a. NAME OF RESPONSIBLE PERSON
a. REPORT	b. ABSTRACT	c. THIS PAGE			STI Help Desk (email: help@sti.nasa.gov)
U	U	U	UU	21	19b. TELEPHONE NUMBER (include area code) 443-757-5802

